



Article

Cryptand-Functionalized Highly Oriented Pyrolytic Graphite Electrodes

Marcos A. Bento ^{1,*}, Sara Realista ^{1,*}, Ana S. Viana ², Ana M. Ferraria ³  and Paulo N. Martinho ^{1,*} 

¹ Biosystems and Integrative Sciences Institute (BioISI), Faculdade de Ciências, Universidade de Lisboa, Campo Grande, 1749-016 Lisboa, Portugal; marcosben31@hotmail.com

² Centro de Química Estrutural, Faculdade de Ciências, Universidade de Lisboa, Campo Grande, 1749-016 Lisboa, Portugal; apsemedo@fc.ul.pt

³ BSIRG, iBB, DEQ, Instituto Superior Técnico, Universidade de Lisboa, Av. Rovisco Pais, 1049-001 Lisboa, Portugal; ana.ferraria@tecnico.ulisboa.pt

* Correspondence: smrealista@fc.ul.pt (S.R.); pnmartinho@fc.ul.pt (P.N.M.)

Abstract: Reproducible materials that have detection properties towards a certain molecule are very important for applications in the fabrication of devices. Among all the substrates that are used, highly oriented pyrolytic graphite allows to clearly image a monolayer. On the other hand, cryptand molecules are versatile because they can sense certain analytes with high selectivity. The highly oriented pyrolytic graphite electrode was first functionalized with an aryl bearing a bromine or an alkyne group to further attach cryptand molecules to its surface. The functionalization was performed through the electroreduction of aryl diazonium salts. While functionalization with an aryl-bromine produced a 20 nm-thick dendritic layer, functionalization of the surface with an aryl bearing a terminal alkyne produced a 9.7 nm-thick multilayer. However, if the diazonium salt is prepared in situ, a 0.9 nm monolayer with aryl-alkyne groups is formed. The alkyne functionalized electrode reacted with a bromo-cryptand through a Sonogashira C–C coupling reaction yielding electrodes functionalized with cryptands. These were immersed in a solution of a Co(II) salt resulting in Co(II)-cryptate modified electrodes, highlighting the ability of the cryptands' modified electrode to sense metal ions. The electrode surface was analyzed by X-ray photoelectron spectroscopy after each modification step, which confirmed the successful functionalization of the substrate with both the cryptand and the cryptate. Cyclic voltammetry studies showed stable current response after approximately six cycles. Different reduction processes were detected for both cryptand (−1.40 V vs. SCE) and cryptate (−1.22 V vs. SCE) modified highly oriented pyrolytic graphite.

Keywords: electrode modification; Sonogashira C–C coupling; cryptand; Co(II) cryptate; monolayer



Citation: Bento, M.A.; Realista, S.; Viana, A.S.; Ferraria, A.M.; Martinho, P.N. Cryptand-Functionalized Highly Oriented Pyrolytic Graphite Electrodes. *Sustainability* **2021**, *13*, 4158. <https://doi.org/10.3390/su13084158>

Academic Editor:
Katsunori Wakabayashi

Received: 9 March 2021

Accepted: 6 April 2021

Published: 8 April 2021

Publisher's Note: MDPI stays neutral with regard to jurisdictional claims in published maps and institutional affiliations.



Copyright: © 2021 by the authors. Licensee MDPI, Basel, Switzerland. This article is an open access article distributed under the terms and conditions of the Creative Commons Attribution (CC BY) license (<https://creativecommons.org/licenses/by/4.0/>).

1. Introduction

The fabrication of materials that can be used as a heterogeneous support with the ability of detecting changes in the substrate is very appealing in terms of developing sensing materials for biological [1], technological [2] or environmental [3] applications. Electrochemistry can play an important role in producing substrates with grafted molecules with recognition sites for different types of guests (e.g., carbon dioxide, anions) [4,5]. These modified substrates have the combined ability of recognition and transducing sensing of target molecules [1]. Electrochemical sensing is an appealing type of signal transduction; however, producing reliable interfaces is still challenging [4].

Several approaches have been used to attach molecules to electrodes, the two main types being chemical and physical [6]. While the physical methods are based on the adsorption of the active molecule on the electrode surface, thus increasing the irreproducibility of the morphologies formed, the chemical methods result in the grafting of the active molecules to the electrode surface [6]. This latter method produces substrates that are less irreproducible and is able to fabricate robust thin films at the monolayer level [7]. Examples

of chemically modified electrodes are the Aramata's Co(II) amino-porphyrin that was immobilized on a glassy carbon (GC) electrode through an amine radical. The GC electrode was first electrochemically modified with an aminopyridyl compound by amine cation radical formation through electrooxidation of the GC in an ethanol solution, followed by chemical bonding of the radical to the GC. This finding showed that recurring to organic chemistry, a molecule can be covalently bound to a substrate producing a modified material (e.g., amide formation, azide-alkyne cycloaddition or diazonium salt electroreduction) [8]. As a result, in 2012 a Co(II) porphyrin was covalently attached to a boron-doped diamond electrode by azide-alkyne cycloaddition reactions. This new electrode exhibited high stability in acetonitrile solutions [9].

Diazonium salts are extremely versatile and have been used to graft compounds onto different substrates, not only by electrochemical [10] but also by chemical [11] methods. This spontaneous grafting method results in the formation of benzene cations that react with different substrates, leading to a covalent attachment to the surface of the substrate [12]. Therefore, due to their unique electronic properties and reactivity, metal complexes have been immobilized on electrodes using electroreduction of diazonium salts [13]. This process can occur either by the formation of the diazonium in situ from a primary amine group [14,15] or by the introduction of a diazonium group on the ligand's structure [16]. The further functionalization of the substrate with a metal complex can be obtained by direct immobilization of the compound or by soaking the ligand-modified electrode in the desired metal salt solution [17]. For example, Fontecave and coworkers [17] immobilized a terpyridine (trpy) ligand on glassy carbon using electroreduction of a diazonium salt in the ligand structure. After immobilization by electrografting, the electrode was soaked in a dimethylformamide (DMF) solution of CoCl_2 , yielding the complex. The same procedure was applied by Jiang et al. [18] and Messerle and coworkers [19], while Nervi and coworkers [20] directly deposited Re(I) and Mn(I) tricarbonyl bipyridine complexes with a diazonium group in the diimine ligand onto the GC electrode. Other complexes were also chemically attached after modifying the electrode surface with an azide [21], amide [22] or carboxylic acid [16] functions.

Although electrografting with aryl diazonium salts has been used to modify surfaces, one of the major drawbacks is the formation of disordered multilayers that can result into poor electron interaction between the electrode and the immobilized compound [21]. Hapiot et al. [10,23] reported the formation of a monolayer but only when aryl diazonium salts with bulkier groups were electrografted onto the electrode. This monolayer allowed further chemical reactions and the formation of a monolayer of a metal complex.

Cryptands and their corresponding metal complexes, cryptates, are versatile supramolecular structures that have proven to be efficient in CO_2 capturing and storage [24] and anion recognition [25]. These preorganized supramolecular structures are key when evaluating their selectivity towards a certain substrate; this has been reviewed by others [26,27]. Following our previous report on CO_2 reduction to CO and CH_4 using a Co(II) cryptate [28], and the proof that cryptands can be stably adsorbed on highly oriented pyrolytic graphite (HOPG) electrode surfaces [29], we investigated the functionalization of HOPG electrodes with cryptands/cryptates, using diazonium salts. Sonogashira coupling reactions based on similar published procedures (e.g., graphene oxide [30] and carbon paper electrodes [31]) were used to immobilize the compounds. These carbon-carbon coupling reactions have been extensively used to prepare many new organic compounds using a terminal alkyne and an aryl or vinyl halide [32]. To the best of our knowledge, this is the first report of a cryptand and cryptate grafted to the surface of an HOPG electrode.

2. Materials and Methods

Atomic force microscopy (AFM) ex situ images were collected in a Multimode atomic force microscope running on the NanoScope IIIa controller (digital instrument Veeco) using tapping mode. To perform the AFM scratch for thickness measurements, a modified method was applied [33]. A first scan was accomplished in tapping mode and after switching for contact mode scans were made in a 500×500 nm with a slow sweep rate (0.5 Hz) and a high deflection force.

For the electrochemical experiments, a potentiostat Autolab PGSTAT 12 AUT71019 controlled by NOVA 2.0 software was used. A three-electrode electrochemical Teflon cell was used with HOPG (active area 0.322 cm^2) and platinum wire was used as working and counter electrodes, respectively. Saturated calomel electrode (SCE = 0.244 V vs. NHE) was used as a reference electrode. Before each experiment to produce a monolayer, the HOPG surface was regenerated by peeling the surface layers using adhesive tape. Before measurements, the solutions were deoxygenated by bubbling N_2 for 20 min. The electrochemical behavior of the modified electrodes was recorded in acetonitrile solution with 0.1 M TBAPF₆ as supporting electrolyte with or without ferrocene (1 mM). Milli-Q water was obtained from a Millipore Milli-Q Gradient Water Purification System.

The X-ray Photoelectron Spectroscopy (XPS) study was performed using an XSAM800 non-monochromatic spectrometer from KRATOS. Operating conditions, spectra acquisition and data treatment were as described elsewhere [34]. The charge shift was corrected using the binding energy of 284.8 eV as reference. The sensitivity factors (SF) used for the quantitative analysis were those of Vision 2 for Windows, Version 2.2.9 from KRATOS, given for Mg K α source. Co 2p_{3/2} SF = 2.33667 was computed for the main component considering the 2p multiplicity of states.

2.1. Potential Cycling Using Synthesized Diazonium Salts (HOPG-Br and HOPG-TMS)

This procedure was based on an existing literature procedure [10]. Modification of the HOPG electrode was performed in a 10 mM solution of the aryl diazonium salt (4-Br-N₂⁺ and 4-TMS-N₂⁺) and 0.1 M TBAPF₆ in acetonitrile using cyclic voltammetry with a scan rate 50 mV s^{-1} during 6 cycles between +0.60 V and −0.75 V vs. SCE. After modification, the electrodes were washed by sonication with acetone and ethanol for 5 min.

2.2. Applying a Reduction Single Step Potential Using 4-TMS-NH₂ (HOPG-TMS)

This procedure was based on a modified literature procedure [15]. The diazonium was produced in situ by the following procedure: in a flask cooled in an ice bath, NaNO₂ (4 equivalents) was added to a 0.1 M HCl solution (10 mL) containing the amine 4-TMS-NH₂ (1 mM). This mixture was left stirring under nitrogen for 5 min. The mixture was then transferred to the Teflon electrochemical cell with the HOPG electrode as the working electrode. After stabilizing for 60 s, a potential of −0.5 V vs. SCE was applied for 30 min. The electrode was washed by sonication for 5 min with water, acetone, ethanol and dichloromethane.

2.3. Silyl Deprotection of HOPG-TMS to HOPG-H

This procedure was based on a literature procedure [10]. The HOPG-TMS electrode was immersed in a 0.05 M tetrabutylammonium fluoride in tetrahydrofuran solution for 30 min. Afterwards, the electrode was thoroughly washed with acetonitrile.

2.4. Sonogashira Coupling for HOPG-Crypt

This was based on a literature procedure [31]. The HOPG-H electrode was immersed in a solution containing copper iodide (12.6 mmol, 2.4 mg), Pd(PPh₃)₄ (12.0 mmol, 13.8 mg), crypt-Br (150 mmol, 0.125 g), distilled triethylamine (45 mmol, 63.6 μL) in 3 mL of anhydrous dimethylformamide previously degassed. This was heated for 30 min at 80 °C. After cooling to room temperature, the electrode was cleaned with acetonitrile by pipetting 4 mL

onto the electrode. This was repeated three times and the electrode was immersed in 8 mL of acetonitrile for one hour. This last cleaning procedure was repeated three times.

2.5. HOPG-Crypt-Co

HOPG-crypt electrode was immersed in a 10 mM $\text{Co}(\text{ClO}_4)_2 \cdot 6\text{H}_2\text{O}$ aqueous solution for four hours, that was previously degassed by bubbling N_2 for 30 min. After this, the electrode was cleaned by immersing the electrode for one hour in Milli-Q water.

3. Results and Discussion

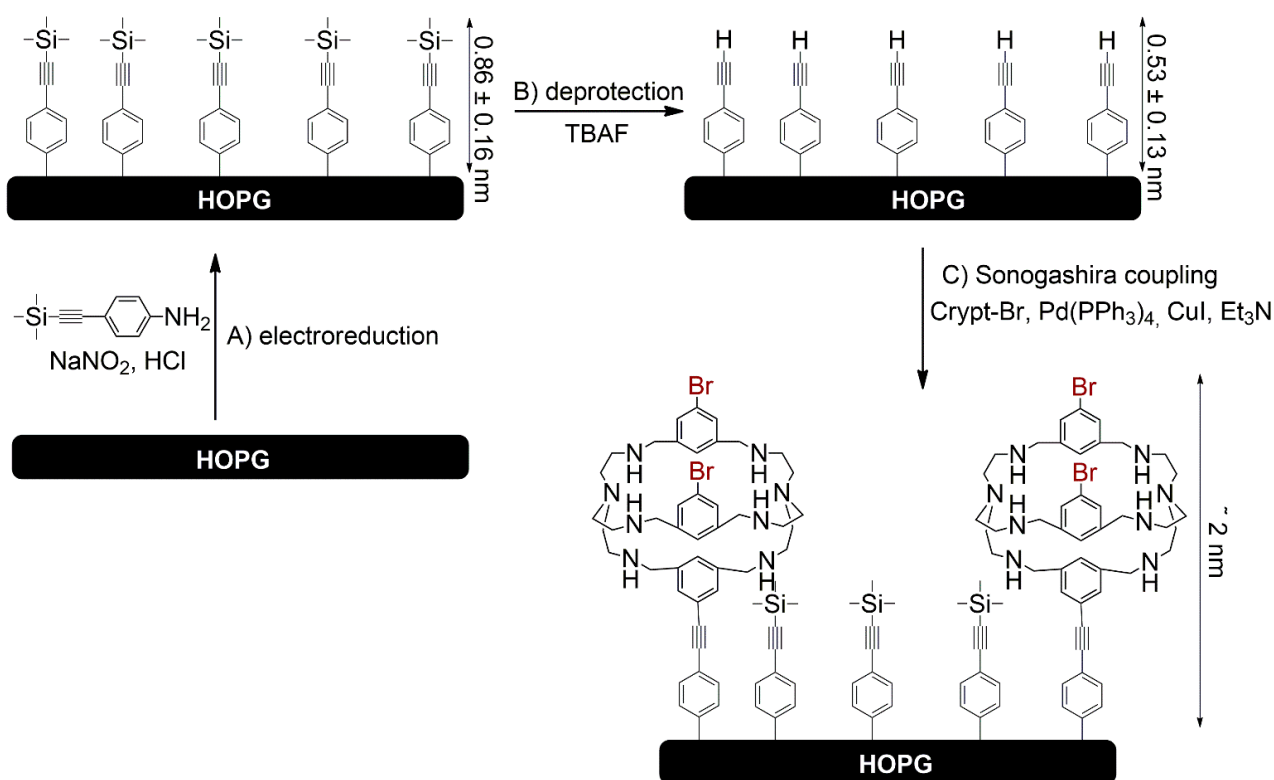
Preparation of the cryptand modified electrodes. To modify electrodes with cryptands, two different approaches of covalent linking using a C–C Sonogashira coupling may be considered (see Supplementary Materials Figure S1, Method A and B). To perform this reaction, the cryptands must have an appropriate aromatic ring substituent: a terminal alkyne (Method A) or a bromine (Method B). The syntheses of both cryptands bearing different aromatic substituents were previously published by our group [28]. These cryptands can be covalently attached to a monolayer produced via the electroreduction of an aryl diazonium salt.

HOPG electrodes were chosen as electrode substrates as they are dominated by edge planes yielding a flat surface with a low roughness, convenient for imaging nanostructures and small modifications in detail (Figure S2) [35]. To follow method A, the compound 4-bromobenzenediazonium tetrafluoroborate (4-Br-N_2^+) was used to produce an aryl bromine monolayer (HOPG-Br, Figure S1) by electroreduction (Figure S3a). This was performed following a literature procedure (Scheme S1) [10]. To study and evaluate the formation of a monolayer onto the electrode surface, the electrochemical behavior of a ferrocene solution (Figure S3b) was analyzed. A loss of reversibility of the redox behavior of ferrocene suggests not only a thicker film than expected but also that the layer presents a high barrier for charge transfer between the molecule and the substrate [36]. The film thickness was determined using AFM with a scratching experiment [33]. This experiment showed a film with 20 nm of thickness (Figure S4) which agrees with the loss of the ferrocene electrochemical behavior. Therefore, through this method a dendritic layer was formed onto the electrode surface and a new method had to be explored to allow monolayer formation [36].

As the purpose of the electrode modification was to obtain an ordered monolayer of cryptands/cryptates, method B was employed as an immobilization strategy. Hapiot et al. [10,23] studied monolayer formation by the electroreduction of silyl capped benzene diazonium salts and observed the prevention of the dendritic growth of the films (Scheme S1). 4-(Trimethylsilyl)ethynylbenzenediazonium tetrafluoroborate (4-TMS-N_2^+) was synthesized [23] and used for electrode monolayer formation using the procedure reported in the literature (Figure S5a,b). The film thickness was also determined by performing an AFM scratch (Figure S5c,d) of the film and crossing a profile section in that region. A thickness of approximately 9.7 nm was obtained that was greater than the thickness reported in the literature (0.86 ± 0.16 nm) [23], indicating the formation of a multilayer.

An alternative approach was attempted by electrografting 4-(trimethylsilyl)ethynylaniline (4-TMS-NH_2) with the formation of the diazonium in situ (Scheme 1). This one-pot electrografting procedure (see materials and methods) was previously reported by others to immobilize a calix[4]arene with an NH_2 function on the aromatic ring [15]. Therefore, this procedure was used to produce a monolayer via generation of diazonium in situ from 4-TMS-NH_2 . The procedure is based on the addition of NaNO_2 to an acidic aqueous solution of 4-TMS-NH_2 , which allows the generation of the diazonium group that after electroreduction leads to a TMS-aryl monolayer. The HOPG electrode was modified with the application of a reductive single step potential (-0.5 vs. SCE) for 30 min (Figure 1a). The electrochemical behavior of a ferrocene solution was investigated by CV (Figure 1b). The cyclic voltammogram (CV) showed similar behavior for ferrocene as that in a bare

HOPG electrode. Their similar response meant that the film formed was not blocking the access to the electrode surface.



Scheme 1. Electroreduction of 4-(trimethylsilyl)ethynylaniline (4-TMS- NH_2) based on a procedure reported in literature [15] for calix[4]arene immobilization. HOPG-TMS deprotection yielding HOPG-H electrode (thickness values from literature [23]). Sonogashira coupling performed on HOPG-H to afford HOPG-crypt (total thickness estimated from the X-ray structure of the cryptand).

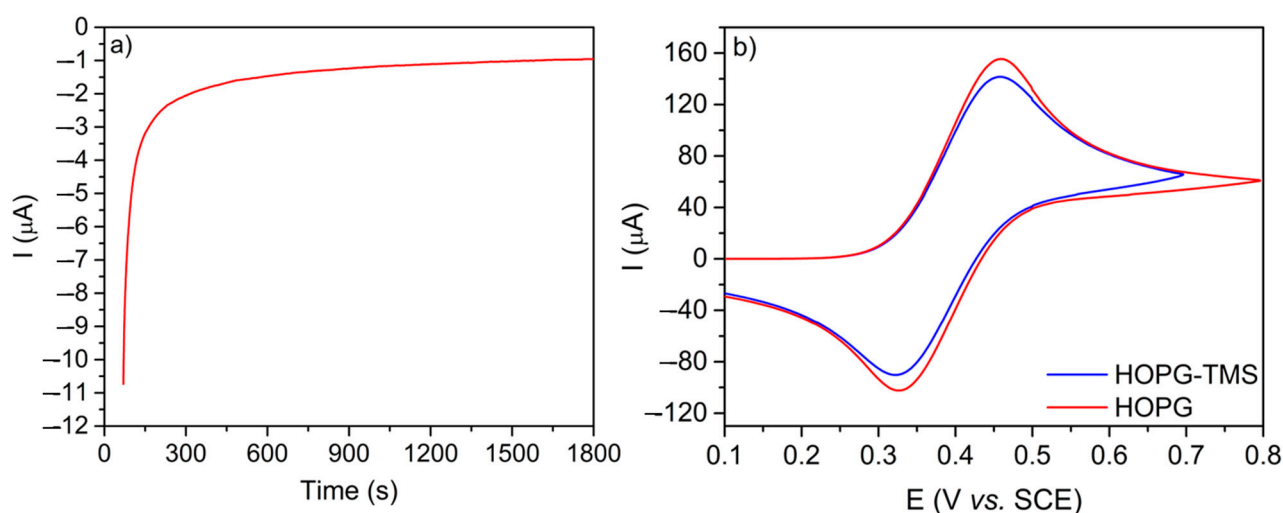


Figure 1. (a) Application of the reductive potential -0.5 V vs. saturated calomel electrode (SCE) for 30 min to a solution containing 4-TMS- NH_2 , NaNO_2 and HCl (diazonium generated in situ) originating HOPG-TMS. (b) Cyclic voltammogram (CV) of 1 mM ferrocene using the HOPG-TMS (blue line) and HOPG (red line) electrodes, 100 mV s^{-1} , 0.1 M TBAPF_6 , CH_3CN . Pt wire and SCE were used as counter and reference electrodes, respectively.

The 2D AFM image shows a different morphology of the film compared to the AFM images obtained for the previous methods, where edges and planes of the HOPG electrode are clearly seen (Figure 2a). The thickness was determined (Figure 2b,c) and is approximately 0.9 nm, which agrees with the literature values for the same type of monolayer [23].

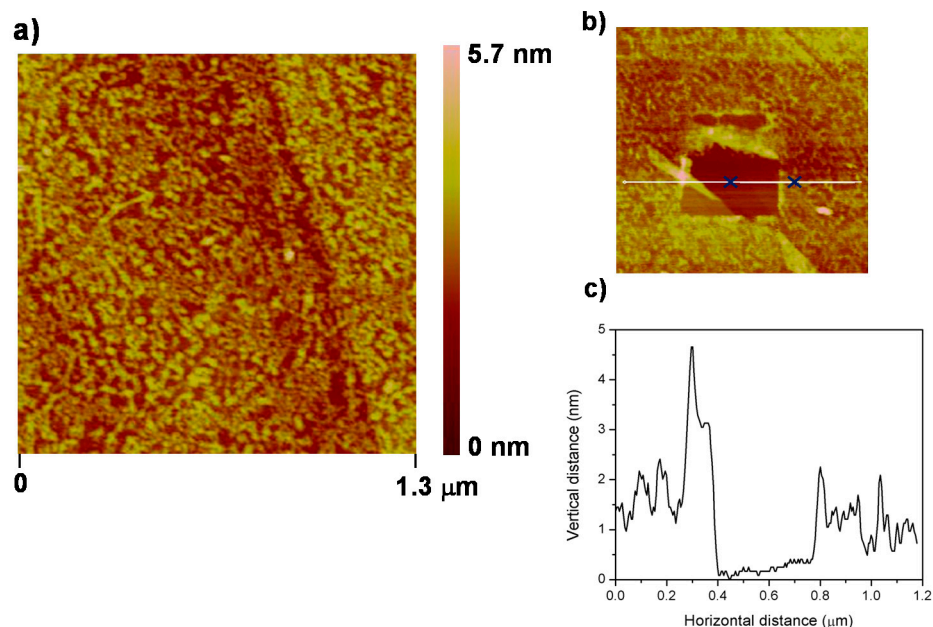


Figure 2. (a) 2D Atomic force microscopy (AFM) image ($1.3\ \mu\text{m} \times 1.3\ \mu\text{m}$) of the HOPG-TMS. (b) $500 \times 500\ \text{nm}$ trench in the monolayer formed with AFM contact mode. (c) Profile section of the AFM scratch to measure film thickness.

After formation of the aryl TMS monolayer, the HOPG-TMS electrode was immersed in a 0.05 M tetrabutylammonium fluoride (TBAF) solution using tetrahydrofuran as solvent following a literature procedure [10] (Scheme 1). This method allows removal of the silyl protective groups, giving rise to a terminal alkyne group (HOPG-H, Scheme 1) where Sonogashira coupling reactions were performed to immobilize the cryptand (Crypt-Br, Figure S1). The procedure for the Sonogashira coupling was based on a previous report where ferrocenes were immobilized on carbon paper electrodes [31].

HOPG-crypt electrodes were analyzed by AFM and a 3D image was compared with a 3D image of HOPG-TMS (Figure S6). The roughness of the HOPG-crypt (Figure S6b) was greater than that of the HOPG-TMS (Figure S6a), which was expected due to the immobilization of the cryptand. Larger and higher globules were detected in HOPG-crypt (Figure S6b) as noted by the higher Z scale used (20 instead of 4.0 nm). The thickness of the HOPG-crypt film was not determined by the same scratch procedure. From the 2D image (Figure 3a) it is possible to observe a rough and heterogeneous surface with several high regions. The thickness varied from 2 to 6 nm of vertical distance (Figure 3a,b) which might be related to the formation of small aggregates with covalently linked molecules and physically adsorbed cryptand molecules that did not get grafted onto the HOPG functionalized surface.

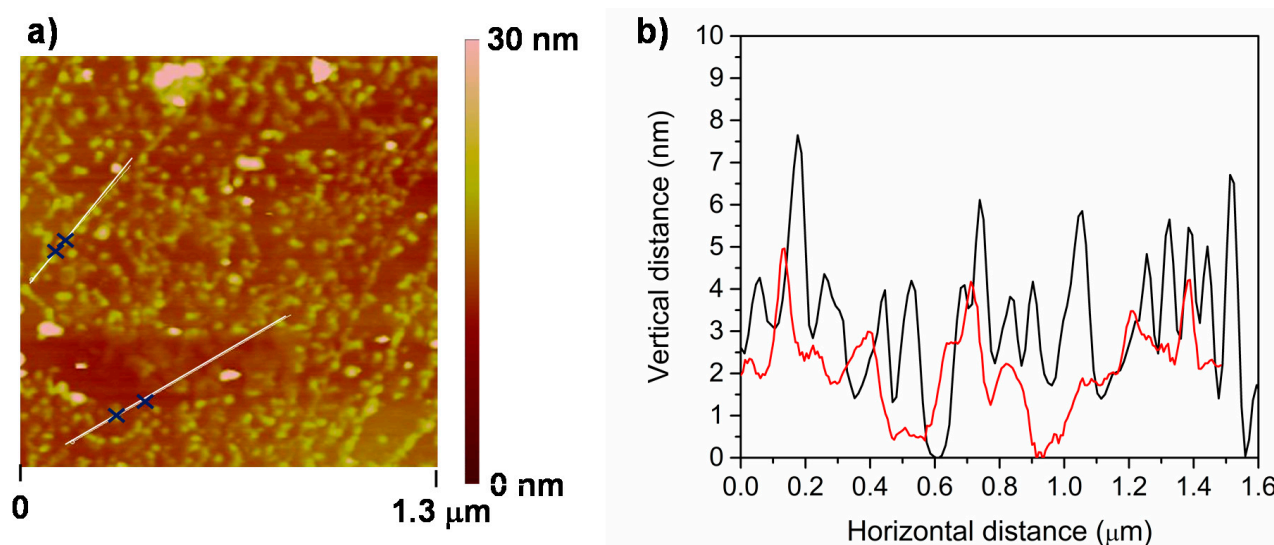


Figure 3. (a) 2D AFM image ($1.3 \times 1.3 \mu\text{m}$) of the HOPG-crypt. (b) Two different profile sections of the HOPG-crypt film.

Electrode surfaces modified by supramolecular structures with sensing ability, in our case cryptands, can turn an inert electrode into a selective material. Cryptands are also versatile in terms of coordinating different metal ions. This results in tuning their selectivity and sensing to capture different types of molecules (e.g., halogens, carbonate, CN^-) [24,37–39]. Thus, our HOPG-crypt was immersed in a 10 mM $\text{Co}(\text{ClO}_4)_2 \cdot 6\text{H}_2\text{O}$ aqueous solution (HOPG-crypt-Co, see materials and methods) and thoroughly washed with water.

The HOPG-crypt and HOPG-crypt-Co were studied under N_2 to characterize the redox processes in the cathodic region (Figure 4). For both samples, the first cycles showed a loss of current which can be associated with material loss. However, after approximately six cycles the current response stabilized, indicating that no further loss of material was occurring. It was possible to observe two distinct reduction processes: one at -1.40 V vs. SCE for the HOPG-crypt and another at -1.22 V vs. SCE for the HOPG-crypt-Co. The latter reduction potential may be identified as the $\text{Co(II)}/\text{Co(I)}$ reduction [40]. Several factors can affect the stability of the electrodes. Among these are the election of solvent (from organic to aqueous), electrolyte and target molecule that will be the subject of further studies. The change in redox behavior before and after coordination of the cobalt ions confirmed the potential of the cryptands to be used as sensors for cations (preferably metals in their lowest oxidation state as nitrogen donor atoms are less hard than oxygen donors). The ability of molecular cryptands to form cryptates with different metals has been shown before and cryptates of Zn(II) , Ni(II) and Cu(II) can be found in the literature. Additionally, due to their cavity dimensions and the distance between the di-metal found therein, these cryptates have also a huge potential to sense analytes in solution, such as the capture of atmospheric CO_2 , cyanide, or halogen anions.

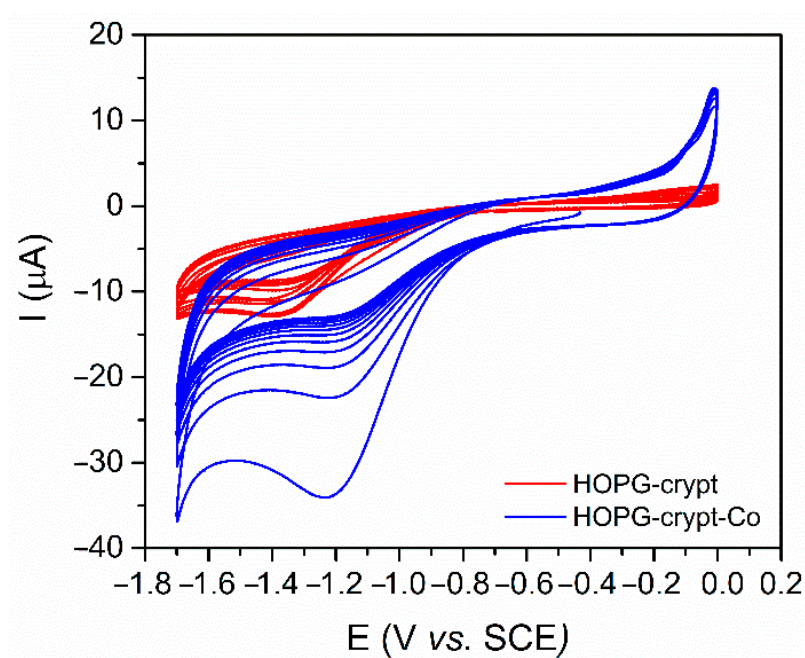


Figure 4. CV of HOPG-crypt (red line) and HOPG-crypt-Co (blue line) under N_2 , 100 mV s^{-1} , 0.1 M TBAPF_6 , CH_3CN . Pt wire and SCE were used as counter and reference electrodes, respectively.

XPS characterization. All the steps of the electrode surface modification were checked by XPS.

Si 2p region (Figure 5a) clearly shows the efficiency of both step 1 and step 2. This region could be fit for both samples with single doublets with a spin-orbit split of 0.61 eV . For the electrode resulting from step 1, HOPG-TMS, the existence of a doublet with the most intense component, Si $2p_{3/2}$, centered at $101.5 \pm 0.2 \text{ eV}$ and assigned to Si bonded to carbons [41], proved that the surface was functionalized with aryl-TMS. After the removal of the silyl protective groups giving rise to a terminal alkyne group (HOPG-H), the signal completely disappeared. However, a small doublet with Si $2p_{3/2}$ centered at $102.7 \pm 0.2 \text{ eV}$ appeared and is assignable to Si bonded to O [42] in silicones, for instance. It may originate in glassware greases and it was also present in subsequent samples.

The third step consisted of a Sonogashira coupling performed on HOPG-H to yield HOPG-crypt. To prove the functionalization, the best way was to rely on the XPS regions Br 3d and N 1s, which should have been found also on the HOPG-crypt-Co sample. Figure 5b,c shows the two regions for both samples. Nitrogen was detected through the photoelectron N 1s. The sample issued from step 2 (HOPG-H) already contained some nitrogen, especially at a binding energy of 403.7 eV . These nitrogen species were in vestigial amounts from precursors used in steps 1 and 2. In step 3, they disappeared, and a large component appeared at $400.4 \pm 0.2 \text{ eV}$ assignable to the cryptand nitrogen atoms. A smaller component at $402.7 \pm 0.2 \text{ eV}$ was assignable to protonated nitrogen [42]. In the HOPG-crypt-Co, the N 1s region was not very different in the position of the main peak but the peak had larger tails, denoting a larger heterogeneity of nitrogen neighborhoods. For the two samples functionalized with cryptands, Br 3d needed two doublets with a spin-orbit split of 1.0 eV . The most intense had the main component, Br $3d_{5/2}$ centered at $71.5 \pm 0.2 \text{ eV}$ and the least intense was centered at $68.9 \pm 0.2 \text{ eV}$. The first one was assigned to the free C(aromatic)-Br. The second one, since it had a lower binding energy, was a species with higher electronic density. It was, maybe, a result of a degradation induced by the X-radiation. They were very similar in both samples. The N/Br atomic ratio computed from the respective areas divided by the sensitivity factors, was 4 in both samples, as expected for the reacted cryptands, proving the successful functionalization in step 3.

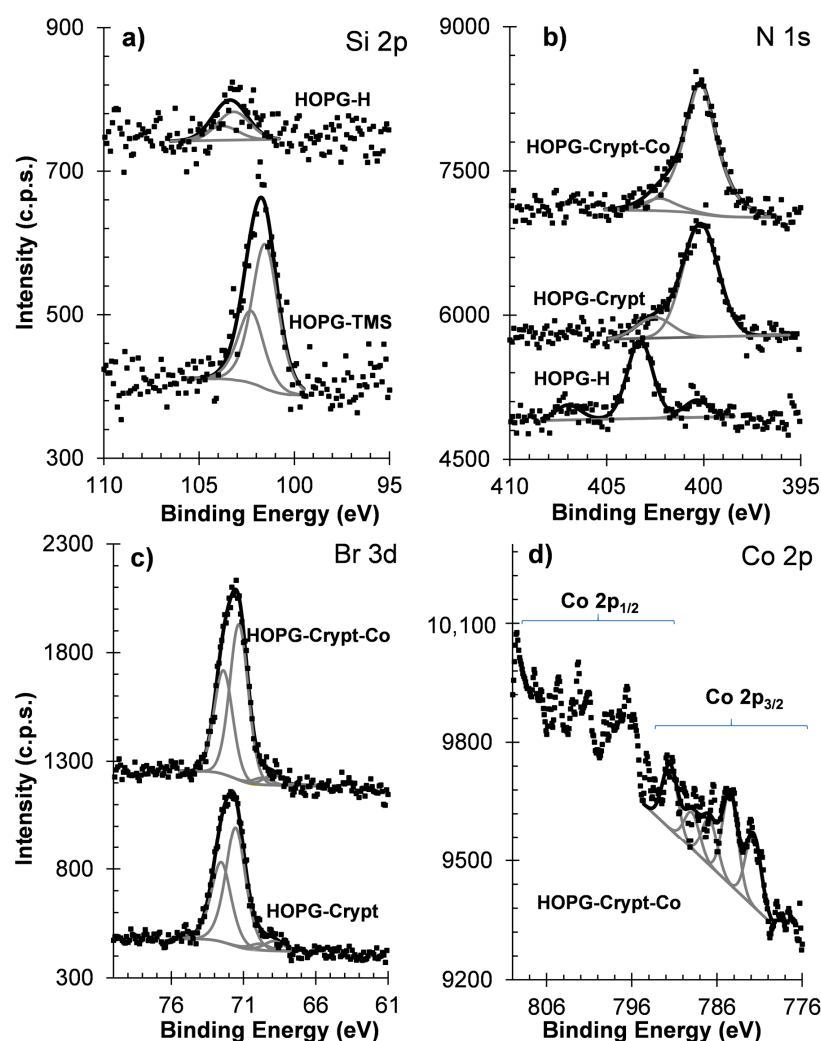


Figure 5. XPS regions (a) Si 2p for HOPG-TMS and for HOPG-H; (b) and (c) N 1s and Br 3d for samples issuing from electrode surface functionalization with cryptands; (d) Co 2p attesting the existence of cobalt in the sample HOPG-Crypt-Co.

Finally, to prove the retention of Co(II) metal center in step 4, the region Co 2p was explored. Figure 5d shows the Co 2p composed by a doublet next to a multiplet structure typical of transition metals with unpaired outer shell electrons. The component centered at lower binding energy, 781.4 eV, has been reported, whether to +2 or +3 oxidation states [41]. From the quantitative point of view, the atomic ratio Co/N was around 0.1. If all the cryptand cavities had Co²⁺ ions, this ratio should be 0.125, which is close to the experimental value.

XPS spectra were also recorded after the CV experiments to confirm the integrity of the films. For that, the XPS spectra for the N 1s and Co 2p regions are shown in Figure S7 and retained the features observed prior to the CV experiments.

4. Conclusions

A HOPG surface was successfully modified with a cryptand via electroreduction of aryl diazonium salts and C–C Sonogashira coupling reactions. The morphology and the thickness of the films produced in each step were imaged by AFM. A monolayer with 0.9 nm thickness was produced on the HOPG surface by electrografting a diazonium salt produced in situ with a bulkier substituent: TMS instead of Br. After the formation of the monolayer and hydrolysis of the TMS group, a terminal alkyne monolayer was obtained. A cryptand with a Br substituent on the aromatic ring (Crypt-Br) was covalently attached

using Sonogashira coupling reaction to the terminal alkyne present in the monolayer. A 2 nm-thickness film was expected but thickness variations from 2–6 nm were obtained which can be related to the pilling of some unreacted cryptands with those grafted on the HOPG surface. This new electrode was submersed in a $\text{Co}(\text{ClO}_4)_2 \cdot 6\text{H}_2\text{O}$ to yield a cryptate modified HOPG. Both cryptand and cryptate modified surfaces were studied by cyclic voltammetry under N_2 and two distinct reduction processes were observed at -1.40 V and -1.22 V (vs. SCE), respectively, the latter being attributed to a $\text{Co(II)}/\text{Co(I)}$ reduction process. Additionally, a stable current response was observed for both modified electrodes after approximately six cycles. XPS confirmed the successful modification performed in each reaction step. It also showed the composition integrity of the modified electrodes before and after the CV experiments. Opportunities to study the ability of the cryptand modified surfaces to sense cations (as shown for Co^{2+}), and the cryptate modified electrodes in CO_2 and anionic analytes, are now possible and will be the subject of further studies in our lab.

Supplementary Materials: The following are available online at <https://www.mdpi.com/article/10.3390/su13084158/s1>. Supplementary material showing a general procedure scheme, AFM images of bare and functionalized HOPG and its functionalization using 4-bromobenzenediazonium tetrafluoroborate and 4-(trimethylsilyl)ethynylbenzenediazonium tetrafluoroborate are shown. XPS spectra after CV studies of HOPG-crypt-Co. Figure S1: Two different methods used for cryptand grafting onto electrodes using C–C Sonogashira coupling. HOPG-Br produced by electroreduction of 4-Br- N_2^+ . HOPG-H is prepared first by electrografting of a diazonium salt formed in situ from 4-TMS- NH_2 , followed by silyl deprotection to yield a terminal alkyne function, Figure S2: 2D AFM image ($2 \times 2 \mu\text{m}$) of an HOPG surface. Figure S3: (a) CV of 10 mM 4-bromobenzenediazonium tetrafluoroborate (4-Br- N_2^+), 6 cycles at 50 mV s^{-1} . (b) CV of 1 mM ferrocene using the modified HOPG-Br and unmodified HOPG electrodes, 100 mV s^{-1} , 0.1 M TBAPF₆, CH_3CN . Pt wire and SCE were used as counter and reference electrodes, respectively. Scheme S1: Electroreduction of the silyl capped benzene diazonium salt 4-(trimethylsilyl)ethynylbenzenediazonium tetrafluoroborate reported by Happtot and coworkers, Figure S4: (a) 2D AFM image ($1 \times 1 \mu\text{m}$) of the modified electrode with 4-Br- N_2^+ . (b) $500 \times 500 \text{ nm}$ trench in the film with AFM contact mode. (c) Profile section of the AFM scratch for film thickness, Figure S5: (a) CV of 10 mM 4-TMS- N_2^+ , 6 cycles at 50 mV s^{-1} , 0.1 M TBAPF₆, CH_3CN . Pt wire and SCE were used as counter and reference electrodes, respectively. (b) 2D AFM image ($3 \times 3 \mu\text{m}$) of the modified electrode. (c) $500 \times 500 \text{ nm}$ trench in the film formed with AFM contact mode. (d) Profile section of the AFM scratch to measure the film thickness, Figure S6: 3D AFM image of (a) HOPG-TMS and (b) HOPG-crypt, Figure S7: XPS regions (a) N 1s and (b) Co 2p of HOPG-crypt-Co after CV.

Author Contributions: Conceptualization: P.N.M. and S.R.; investigation: M.A.B., S.R. and A.S.V.; resources: P.N.M., A.M.F. and A.S.V.; data curation: S.R. and P.N.M.; writing—original draft preparation: P.N.M. and S.R.; writing—review & editing: M.A.B., P.N.M., A.M.F., A.S.V. and S.R.; supervision: S.R. and P.N.M.; project administration: P.N.M. All authors have read and agreed to the published version of the manuscript.

Funding: This research received no external funding.

Institutional Review Board Statement: Not applicable.

Informed Consent Statement: Not applicable.

Data Availability Statement: Not applicable.

Acknowledgments: We thank the Fundação para a Ciência e a Tecnologia, Portugal, for financial support (UID/MULTI/00612/2019, UID/MULTI/04046/2019 and UIDB/04565/2020) and project PTDC/QEQQIN/3414/2014. S.R. thanks FCT for fellowship (PD/BD/52368/2013) under the CAT-SUS doctoral program. P.N.M. thanks FTC for the program CEECIND/00509/2017. We are thankful for the contribution of Ana M. Rego from IST to the XPS study.

Conflicts of Interest: The authors declare no conflict of interest.

References

- Maduraiveeran, G.; Sasidharan, M.; Ganesan, V. Electrochemical sensor and biosensor platforms based on advanced nanomaterials for biological and biomedical applications. *Biosens. Bioelectron.* **2018**, *103*, 113–129. [\[CrossRef\]](#) [\[PubMed\]](#)
- Schroeder, T.B.H.; Houghtaling, J.; Wilts, B.D.; Mayer, M. It's Not a Bug, It's a Feature: Functional Materials in Insects. *Adv. Mater.* **2018**, *30*, 1705322. [\[CrossRef\]](#)
- Joshi, A.; Kim, K.-H. Recent advances in nanomaterial-based electrochemical detection of antibiotics: Challenges and future perspectives. *Biosens. Bioelectron.* **2020**, *153*, 112046. [\[CrossRef\]](#)
- Elique, A.; Etard, B.; Fischer, R.A. Metal-Organic Framework Thin Films: From Fundamentals to Applications. *Chem. Rev.* **2011**, *112*, 1055–1083.
- Hein, R.; Beer, P.D.; Davis, J.J. Electrochemical Anion Sensing: Supramolecular Approaches. *Chem. Rev.* **2020**, *120*, 1888–1935. [\[CrossRef\]](#)
- Alam, M.T.; Gooding, J.J. Modification of Carbon Electrode Surfaces. In *Advances in Electrochemical Science and Engineering*; Wiley: Hoboken, NJ, USA, 2015; Volume 16, pp. 211–240.
- Li, F.; Yang, H.; Li, W.; Sun, L. Device Fabrication for Water Oxidation, Hydrogen Generation, and CO₂ Reduction via Molecular Engineering. *Joule* **2018**, *2*, 36–60. [\[CrossRef\]](#)
- Tanaka, H.; Aramata, A. Aminopyridyl cation radical method for bridging between metal complex and glassy carbon: Cobalt(II) tetraphenylporphyrin bonded on glassy carbon for enhancement of CO₂ electroreduction. *J. Electroanal. Chem.* **1997**, *437*, 29–35. [\[CrossRef\]](#)
- Yao, S.A.; Ruther, R.E.; Zhang, L.; Franking, R.A.; Hamers, R.J.; Berry, J.F. Covalent attachment of catalyst molecules to conductive diamond: CO₂ reduction using “smart” electrodes. *J. Am. Chem. Soc.* **2012**, *134*, 15632–15635. [\[CrossRef\]](#)
- Leroux, Y.R.; Fei, H.; Noël, J.M.; Roux, C.; Hapiot, P. Efficient covalent modification of a carbon surface: Use of a silyl protecting group to form an active monolayer. *J. Am. Chem. Soc.* **2010**, *132*, 14039–14041. [\[CrossRef\]](#)
- Maurin, A.; Robert, M. Catalytic CO₂-to-CO conversion in water by covalently functionalized carbon nanotubes with a molecular iron catalyst. *Chem. Commun.* **2016**, *52*, 12084–12087. [\[CrossRef\]](#)
- Mesnage, A.; Lefèvre, X.; Jégou, P.; Deniau, G.; Palacin, S. Spontaneous Grafting of Diazonium Salts: Chemical Mechanism on Metallic Surfaces. *Langmuir* **2012**, *28*, 11767–11778. [\[CrossRef\]](#)
- Bullock, R.M.; Das, A.K.; Appel, A.M. Surface Immobilization of Molecular Electrocatalysts for Energy Conversion. *Chem. Eur. J.* **2017**, *23*, 7626–7641. [\[CrossRef\]](#)
- Lyskawa, J.; Bélanger, D. Direct modification of a gold electrode with aminophenyl groups by electrochemical reduction of in situ generated aminophenyl monodiazonium cations. *Chem. Mater.* **2006**, *18*, 4755–4763. [\[CrossRef\]](#)
- Santos, L.; Mattiuzzi, A.; Jabin, I.; Vandencastele, N.; Reniers, F.; Reinaud, O.; Hapiot, P.; Lhenry, S.; Leroux, Y.; Lagrost, C. One-pot electrografting of mixed monolayers with controlled composition. *J. Phys. Chem. C* **2014**, *118*, 15919–15928. [\[CrossRef\]](#)
- Jane, R.T.; Gaudemer, E.; Lomoth, R. Surface modification of carbon and metal electrodes with bistable molecular redox switches by click and amide coupling. *J. Mater. Chem. C* **2015**, *3*, 10023–10030. [\[CrossRef\]](#)
- Elgrishi, N.; Griveau, S.; Chambers, M.B.; Bedioui, F.; Fontecave, M. Versatile functionalization of carbon electrodes with a polypyridine ligand: Metallation and electrocatalytic H⁺ and CO₂ reduction. *Chem. Commun.* **2015**, *51*, 2995–2998. [\[CrossRef\]](#) [\[PubMed\]](#)
- Laviron, E. A multilayer model for the study of space distributed redox modified electrodes. *J. Electroanal. Chem. Interfacial Electrochem.* **1980**, *112*, 1–9. [\[CrossRef\]](#)
- Tregubov, A.A.; Vuong, K.Q.; Luais, E.; Gooding, J.J.; Messerle, B.A. Rh(I) complexes bearing N,N and N,P ligands anchored on glassy carbon electrodes: Toward recyclable hydroamination catalysts. *J. Am. Chem. Soc.* **2013**, *135*, 16429–16437. [\[CrossRef\]](#)
- Sun, C.; Rotundo, L.; Garino, C.; Nencini, L.; Yoon, S.S.; Gobetto, R.; Nervi, C. Electrochemical CO₂ Reduction at Glassy Carbon Electrodes Functionalized by MnI and ReI Organometallic Complexes. *ChemPhysChem* **2017**, *18*, 3219–3229. [\[CrossRef\]](#) [\[PubMed\]](#)
- Zhang, L.; Vilà, N.; Kohring, G.W.; Walcarius, A.; Etienne, M. Covalent Immobilization of (2,2'-Bipyridyl) (Pentamethylcyclopentadienyl)-Rhodium Complex on a Porous Carbon Electrode for Efficient Electrocatalytic NADH Regeneration. *ACS Catal.* **2017**, *7*, 4386–4394. [\[CrossRef\]](#)
- O'Donoghue, C.S.J.N.; Shumba, M.; Nyokong, T. Electrode Modification through Click Chemistry Using Ni and Co Alkyne Phthalocyanines for Electrocatalytic Detection of Hydrazine. *Electroanalysis* **2017**, *29*, 1731–1740. [\[CrossRef\]](#)
- Leroux, Y.R.; Hapiot, P. Nanostructured monolayers on carbon substrates prepared by electrografting of protected aryldiazonium salts. *Chem. Mater.* **2013**, *25*, 489–495. [\[CrossRef\]](#)
- Dussart, Y.; Harding, C.; Dalgaard, P.; McKenzie, C.; Kadirvelraj, R.; McKee, V.; Nelson, J. Cascade chemistry in azacryptand cages: Bridging carbonates and methylcarbonates. *J. Chem. Soc. Dalton Trans.* **2002**, 1704–1713. [\[CrossRef\]](#)
- Alibrandi, G.; Amendola, V.; Bergamaschi, G.; Fabbri, L.; Licchelli, M. Bistren cryptands and cryptates: Versatile receptors for anion inclusion and recognition in water. *Org. Biomol. Chem.* **2015**, *13*, 3510–3524. [\[CrossRef\]](#) [\[PubMed\]](#)
- Deraedt, C.; Astruc, D. Supramolecular nanoreactors for catalysis. *Coord. Chem. Rev.* **2016**, *324*, 106–122. [\[CrossRef\]](#)
- Delgado-Pinar, E.; García-España, E.; Verdejo, B.; Pitarch-Jarque, J. Metal Complexes as Receptors. In *Comprehensive Supramolecular Chemistry II*; Elsevier Inc.: Amsterdam, The Netherlands, 2017; Volume 3, pp. 437–477.
- Realista, S.; Almeida, J.C.; Milheiro, S.A.; Bandeira, N.A.G.; Alves, L.G.; Madeira, F.; Calhorda, M.J.; Martinho, P. Co(II) cryptates convert CO₂ into CO and CH₄ under visible light. *Chem. Eur. J.* **2019**, *25*, 11670–11679. [\[CrossRef\]](#)

-
29. Markey, L.; Stievenard, D.; Devos, A.; Lannoo, M.; Demol, F.; de Backer, M. STM observations of self-assembled 1D and 2D nanoclusters of aromatic cryptand molecules deposited on highly oriented pyrolytic graphite. *Supramol. Sci.* **1997**, *4*, 375–379. [[CrossRef](#)]
 30. Pramoda, K.; Kumar, R.; Rao, C.N.R. Graphene / Single-Walled Carbon Nanotube Composites Generated by Covalent Cross-Linking. *Chem. Asian J.* **2015**, *10*, 2147–2152. [[CrossRef](#)]
 31. Gietter, A.A.S.; Pupillo, R.C.; Yap, G.P.A.; Beebe, T.P.; Rosenthal, J.; Watson, D.A. On-surface cross-coupling methods for the construction of modified electrode assemblies with tailored morphologies. *Chem. Sci.* **2013**, *4*, 437–443. [[CrossRef](#)] [[PubMed](#)]
 32. Sonogashira, K. Development of Pd–Cu catalyzed cross-coupling of terminal acetylenes with sp²-carbon halides. *J. Organomet. Chem.* **2002**, *653*, 46–49. [[CrossRef](#)]
 33. Anariba, F.; DuVall, S.H.; McCreery, R.L. Mono- and Multilayer Formation by Diazonium Reduction on Carbon Surfaces Monitored with Atomic Force Microscopy “Scratching”. *Anal. Chem.* **2003**, *75*, 3837–3844. [[CrossRef](#)] [[PubMed](#)]
 34. Tsyganov, D.; Bundaleska, N.; Henriques, J.; Felizardo, E.; Dias, A.; Abrashev, M.; Kissovski, J.; Botelho do Rego, A.M.; Ferraria, A.M.; Tatarova, E. Simultaneous Synthesis and Nitrogen Doping of Free-Standing Graphene Applying Microwave Plasma. *Materials* **2020**, *13*, 4213. [[CrossRef](#)]
 35. Patel, A.N.; Collignon, M.G.; O’connell, M.A.; Hung, W.O.Y.; Mckelvey, K.; Macpherson, J.V.; Unwin, P.R. A New View of Electrochemistry at Highly Oriented Pyrolytic Graphite. *J. Am. Chem. Soc.* **2012**, *134*, 20117–20130. [[CrossRef](#)]
 36. Müri, M.; Gotsmann, B.; Leroux, Y.; Trouwborst, M.; Lörscher, E.; Riel, H.; Mayor, M. Modular functionalization of electrodes by cross-coupling reactions at their surfaces. *Adv. Funct. Mater.* **2011**, *21*, 3706–3714. [[CrossRef](#)]
 37. Zhong, D.C.; Lu, T.B. Molecular recognition and activation by polyaza macrocyclic compounds based on host-guest interactions. *Chem. Commun.* **2016**, *52*, 10322–10337. [[CrossRef](#)] [[PubMed](#)]
 38. Möller, F.; Merz, K.; Herrmann, C.; Apfel, U.-P. Bimetallic nickel complexes for selective CO₂ carbon capture and sequestration. *Dalton Trans.* **2016**, *45*, 904–907. [[CrossRef](#)]
 39. Amendola, V.; Bergamaschi, G.; Miljkovic, A. Azacryptands as molecular cages for anions and metal ions. *Supramol. Chem.* **2018**, *30*, 236–242. [[CrossRef](#)]
 40. Ouyang, T.; Huang, H.; Wang, J.; Zhong, D.; Lu, T. A Dinuclear Cobalt Cryptate as a Homogeneous Photocatalyst for Highly Selective and Efficient Visible-Light Driven CO₂ Reduction to CO in CH₃CN/H₂O Solution. *Angew. Chem. Int. Ed.* **2017**, *56*, 738–743. [[CrossRef](#)]
 41. NIST X-ray Photoelectron Spectroscopy (XPS) Database, Version 3.5. Available online: <https://srdata.nist.gov/xps/> (accessed on 2 March 2021).
 42. Nunes, B.; Franco, N.; Botelho Do Rego, A.M.; Alves, E.; Colaço, R. Structural characterization of dual ion implantation in silicon. *Nucl. Instrum. Methods Phys. Res. Sect. B Beam Interact. Mater. Atoms* **2015**, *365*, 39–43. [[CrossRef](#)]